2-25-2019

Mechanical behaviors of hydrogel-impregnated sand

Kejun Wen
Jackson State University

Yang Li
Jackson State University

Wei Huang
Chongqing University of Science and Technology

Catherine Armwood
Tennessee State University

Farshad Amini
Jackson State University

See next page for additional authors

Recommended Citation

Kejun Wen, Yang Li, Wei Huang, Catherine Armwood, Farshad Amini, Lin Li, "Mechanical behaviors of hydrogel-impregnated sand", Construction and Building Materials, Volume 207, 2019, Pages 174-180, ISSN 0950-0618, https://doi.org/10.1016/j.conbuildmat.2019.02.141.

Authors
Kejun Wen, Yang Li, Wei Huang, Catherine Armwood, Farshad Amini, and Lin Li

Mechanical behaviors of hydrogel-impregnated sand

Kejun Wen[a], Yang Li[b], Wei Huang[c], Catherine Armwood[d], Farshad Amini[e], Lin Li[f]

Abstract: Hydrogel has been widely used in medical studies due to their unique integration of solid and liquid properties. There is limited studies of using hydrogel in construction materials. The goal of this study was to investigate the effect of hydrogel on mechanical behaviors of sandy materials. The effects of reaction time, sodium alginate content, and curing temperature on mechanical behaviors of hydrogel-impregnated sand were studied through unconfined compression tests, falling head permeability tests, consolidated and undrained triaxial tests, scanning electron microscopy, and durability tests. The unconfined compression strength (UCS) increased with sodium alginate content, but the hydraulic conductivity of hydrogel-impregnated sand decreased with sodium alginate content. The optimum reaction time and curing temperature were found to be 3 days and 50°C, respectively, for the hydrogel-impregnated sand. The stress-strain curves of hydrogel-impregnated sand indicated that the ductility of hydrogel-impregnated sand was significantly improved compared with the traditional cementitious method. Moreover, the results of durability tests indicated that approximately 60% of the original UCS of hydrogel-impregnated sand still remained after 12 wet-dry and freeze-thaw cycles.

Keywords: Hydrogel, Ductility, Curing condition, Wet-dry, Freeze-thaw

[a] Research Associate, Department of Civil and Environmental Engineering, Jackson State University, 1400 John R. Lynch St., Jackson, MS 39217, USA.
[b] Research Associate, Department of Civil and Environmental Engineering, Jackson State University, 1400 John R. Lynch St., Jackson, MS 39217, USA.
[c] Assistant Professor, School of Civil Engineering and Architecture, Chongqing University of Science and Technology, Chongqing 401331, China.
[d] Assistant Professor, Department of Civil and Architectural Engineering, Tennessee State University, 3500 John A. Merritt Boulevard, Nashville TN 37209, USA.
[e] Professor, Department. of Civil and Environmental Engineering, Jackson State University, 1400 John R. Lynch St., Jackson, MS 39217, USA.
[f] Professor, Department of Civil and Architectural Engineering, Tennessee State University, 3500 John A. Merritt Boulevard, Nashville TN 37209, USA; 615-963-5417, lli1@tnstate.edu, corresponding author.

Introduction

Mechanical and chemical treatment methods have been developed to improve soil properties of strength, erosion, dynamic resistance, and stability [1]. The mechanical treatment methods include densification, dewatering, and structural reinforcement [2-4]. The chemical treatment methods involve chemical stabilizers such as cement, lime, fly ash, gypsum, and bituminous materials [5-7]. The stabilization mechanisms of chemical treatments have been extensively studied [8-11]. However, these materials are costly and may have environmental concerns [1]. These additives may cause the increase of soil pH after treatment, which have negative effects on surrounding groundwater and plants. Moreover, the treated soils commonly exhibit brittle behavior that potentially affect their stability for structures [11,12]. Meanwhile, the production of traditional additives, such as cement and lime, consume a large amount of natural resources and energy [1]. Therefore, the development of eco-friendly materials for soil improvement is essential.

Non-traditional additives including enzymes, microbials, resins, acids, and polymers have gained much attention in recent years [13-15]. The bio-geochemical processes that induces mineral precipitation, has been utilized as an alternative to traditional chemical grouting [16]. Microbial induced calcite precipitation (MICP) is the most common bio-process that has been studied. The MICP treatment requires the existence of ureolytic bacteria, urea, and calcium-rich solution to drive the bio-geochemical reaction [13,17,18,19]. The MICP treatment helps bond the soil particles of sand to improve the mechanical behavior of sandy soil. The MICP-treated sand materials have been applied as alternative construction materials in the development of bio-bricks and bio-beams [11,16,19]. Wen et al. [19] found that the flexure strength of bio-beams could achieve around 3.0 MPa, which is equivalent to a plain concrete beams. However, the

MICP-treated sand materials exhibit brittle performance which is opposite of the desired ductile performance needed for beams [11,19]. Recent studies have shown that using gel-type bio-polymers can possibly improve the soil strength and the ductility of sandy soil [20]. Previous studies mostly focused on the use of thermo-gelation bio-polymer such as gellan and agar biopolymers, which require a high temperature (~100℃) during the reaction. Chang et al. [20] mixed sand with gellan gum at 100°C and tested the UCS after sample cooling. The test results showed that the 2% gellan gum-treated sand gained around 400 kPa UCS and failed at 7% strain when the sample fully dried. However, the sample lost almost 90% strength after re-submerging the sample into water. The durability of biopolymer-treated soil presents to be unstable in aqueous environments.

Hydrogel, a class of three-dimensional (3D) networks formed through the cross-linking of hydrophilic polymer chains embedded in a water-rich environment, possesses broadly tunable physical and chemical properties [21,22]. Hydrogel is abundant in plant and animal tissue, with examples ranging from xylems and phloems to muscles and cartilages [23]. Due to their unique integration of solid and liquid properties, hydrogel has been widely explored in diverse application such as drug delivery, biomedicine, soft electronics, sensors, tissue engineering, and coating for medical devices [22,23,24]. Gong et al. [24] developed a strong hydrogel by inducing the double-network structure method. The double-network structure with poly (2-acrylamido-2-methylpropanesulfonic acid) and poly (acrylamide) hydrogel can sustain a compression stress of 17.2 MPa and recover immediately after unloading. Sun et al. [25] developed a synthetic hydrogel by mixing Ca-alginate and polyacrylamide to achieve tough and stretchable properties. The alginate-polyacrylamide hybrid gel can be stretched to exceed 20 times its original length

without rupture. The superior toughness and mechanical strength of hydrogel has the potential to improve the ductility and dynamic loading resistance of construction materials.

The goal of this study was to apply Ca-alginate hydrogel for improving the ductility and mechanical behavior of sandy soil. In this study, the Ca-alginate hydrogel was selected due to its environmentally friendly properties [26,27]. The effects of reaction time, sodium alginate content, and curing temperature on mechanical behaviors of hydrogel-impregnated sand were studied through unconfined compression tests, falling head permeability tests, consolidated and undrained triaxial tests, scanning electron microscopy, and durability tests.

Materials and Methods

Sand

Mississippi local sand was used in this study. The sieve analysis method was used to determine the sand particle size distributions according to ASTM C136 [28]. The standard U.S. sieve was used in this study. The sand particle distribution curve is shown in Figure 1. The coefficient of uniformity (C_u) and gradation (C_c) were determined as 2.05 and 1.21, respectively. It was classified as a poorly graded sand (SP) according to Unified Soil Classification System (USCS).

Ca-alginate Hydrogel

The Ca-alginate hydrogel was prepared from sodium alginate solution that mixing the solution with $CaCl_2$ agents [29]. The sodium alginate was delivered as powder and the gel solution was created when the powders were mixed with water. The sodium alginate powder used in this study was supplied by ACRON (CAS No. 9005-38-3). The sodium alginate solutions were prepared in DI water at room temperature. Four different sodium alginate contents (0.1%, 0.2%, 0.3% and 0.4% by weight of dry sand) were used for this study.

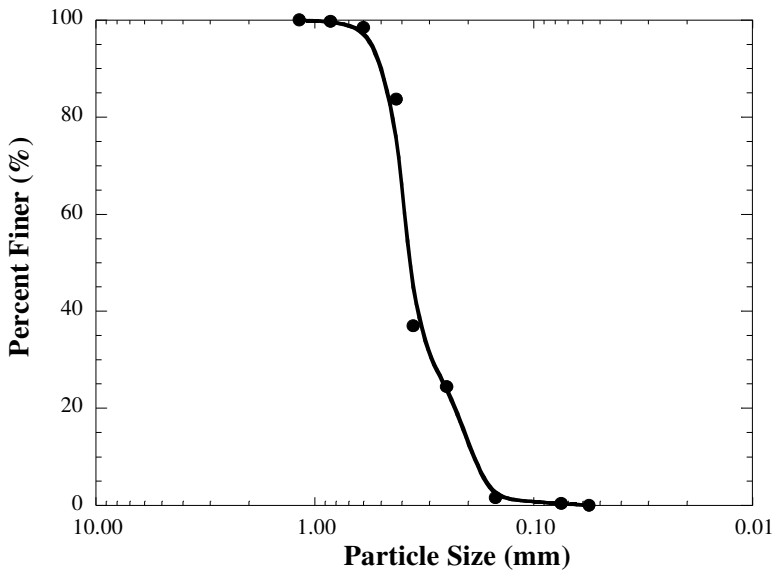

Figure 1. Particle distribution curve of Mississippi sand.

Hydrogel-impregnated Sample Preparation

All hydrogel-impregnated sand samples were prepared using the following sample preparation method. Sodium alginate solution (~20 mL) was mixed with sand (100 g) to a workable status at room temperature as shown in Figure 2 (a). The mixture was compacted in a mini compaction mold with a diameter of 33.0 mm (1.3 in.) and a height of 71.1 mm (2.8 in.) (Figure 2 (b)). After compaction, the sample was extruded out and merged into 0.5 M $CaCl_2$ solution as shown in Figure 2 (c). The $CaCl_2$ solution was used as ionic cross-linking agent with sodium alginate to form the Ca-alginate hydrogel. The formatted Ca-alginate hydrogel can cement the sand particles together and improve the mechanical performance of sand. Different reaction times (1, 3, 5, 7, 14, 28 days) in the $CaCl_2$ solution were investigated to explore the optimum performance of hydrogel-impregnated sand. All testing samples were prepared in triplicate.

Four different curing conditions were selected to investigate the effect of curing temperature on the properties of hydrogel-impregnated sand. After removing the samples from the reaction tank, the hydrogel-impregnated sand was either (1) air-dried at room temperature (25^0C) for 28 days, (2) oven-dried in 50^0C for 24 h, (3) oven-dried in 80^0C for 24 h, or (4) oven-dried in 100^0C for 24 h.

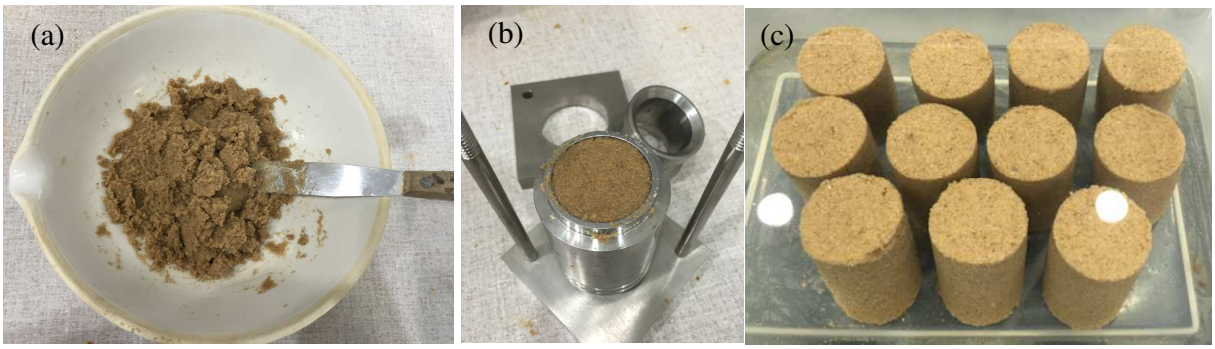

Figure 2. Images of sample preparation.

Unconfined Compression Test

The hydrogel-impregnated samples for the unconfined compression test were cylinder-shaped with 2H:1D ratio (diameter of 33.0 mm and height of 71.1 mm). The unconfined compression test was conducted under strain-controlled conditions at a uniform loading rate of 1.5%/min in accordance with ASTM D2166 [30].

Permeability Test

The falling head permeability testing method was used to test the hydraulic conductivity of the hydrogel-impregnated sand following ASTM D5084-16a [31]. For untreated sand, the constant head permeability testing method was used following ASTM D2434-68 [32].

Consolidated and Undrained Triaxial Test

Consolidation undrained triaxial compression tests were conducted under 100, 200 and 400 kPa cell pressure at a constant axial strain rate of 1.0% stain/min. The tests terminated after the strain reached 15%.

Durability tests

Durability tests of hydrogel-impregnated sample were conducted in accordance with ASTM D 560 [33] for freeze-thaw cycles and ASTM D 559 [34] for wet-dry cycles. The UCS tests were conducted on these samples after every 3 cycles.

Freeze-thaw

Every freeze-thaw cycle began by introducing specimens in a freezing cabinet with constant temperature of -23^{0}C for 24 h. Next, the samples were placed in the moist room at temperature of 25^{0}C and a relative humidity of 100% for 24 h. The number of freeze-thaw cycles was up to 12 times in this study. The mass loss after each freeze-thaw cycle were measured. After each freeze-thaw cycle, the hydrogel-impregnated samples were thawed at 50^{0}C for 24 h before testing.

Wet-dry

Every wet-dry cycle began with oven drying for 24 h at 50^{0}C. Then, specimens were immersed underwater for 24 h at 25^{0}C. The number of wet-dry cycles was up to 12 times in this study. The mass loss after each wet-dry cycle were measured.

Scanning Electron Microscopy (SEM) Analysis

SEM images were taken to observe the micro-scale connections between hydrogel and sand particles. Selected samples including untreated sand and hydrogel-impregnated sand under wet

138 and dry conditions were mounted on the stubs with adhesive carbon conductive tabs. The
139 prepared samples were observed by secondary electron detection in SEM (TESCAN LYRA3).
140

141 **Results and Discussion**

142 ***Effect of reaction time on strength improvement of hydrogel-impregnated sand***

143 The stress-strain relationship of hydrogel-impregnated sand with 0.4% sodium alginate content at
144 different reaction times (1 day, 3 day, 5 day, 7 day, and 14 days) in the $CaCl_2$ solution is shown
145 in Figure 3. The conventionally-reinforced sandy soil commonly exhibited a brittle behavior
146 [11,17]. In contrast, the failure stain of hydrogel-impregnated sand could reach up to 6%,
147 indicating a good ductility behavior. Meanwhile, all samples exhibited residual strength after the
148 peak strength, which demonstrated better elastic behavior. The UCS of hydrogel-impregnated
149 sand increased with reaction time up to 3 days, and then the UCS started to reduce. This could be
150 caused by the degradation or decrosslinking of hydrogel. Shoichet et al. [35] found that increased
151 exposure of calcium-crosslinked alginate to sodium citrate can result in decreased gel strength
152 because sodium citrate chelates calcium, thereby decrosslinking calcium alginate. Rowley et al.
153 [36] also indicated that the ionically crosslinked alginates lost its mechanical properties over
154 time due to an outward flux of crosslinking ions into the surrounding medium. The exchange
155 between divalent crosslinking ions (e.g., Ca^{2+}) with monovalent ions from the surrounding
156 environment causes alginate hydrogels to degrade [37]. In this study, the sodium ions in the
157 solution may have degraded the Ca-alginate over time. Therefore, the study proposed the
158 optimum reaction time for Ca-alginate was 3 days.

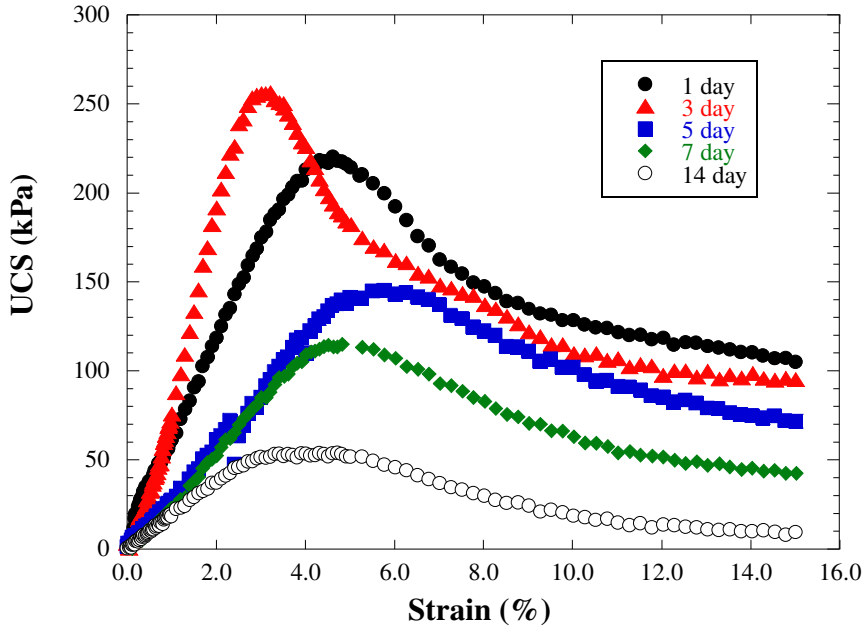

Figure 3. The UCS of hydrogel-impregnated sand with 0.4% sodium alginate content at different reaction times.

Effect of sodium alginate content on strength improvement of hydrogel-impregnated sand

The stress-strain relationship of hydrogel-impregnated sand at different sodium alginate contents after 3 days of reaction time was shown in Figure 4 (a). It can be seen that the UCS of hydrogel-impregnated sand increased with the increase of sodium alginate content. The strength of hydrogel-impregnated sand at 0.4% sodium alginate content (260 kPa) was around two times higher than that at 0.1% sodium alginate content (140 kPa). Bu et al. [11] found that the UCS of the optimum lime-treated sand (15% by weight of dry sand) was 140 kPa, which is similar to hydrogel-impregnated sand with 0.1% sodium alginate. The UCS of hydrogel-impregnated sand was lower than that of cement-treated sand, but is still comparable with a lower percentage additive at 0.4%. Consoli et al. [38] reported that the UCS of 2% cement-treated sand was around 250 kPa which was similar to that of hydrogel-impregnated sand with 0.4% sodium alginate. Chang et al. [12] mixed different contents of gellan gum with sand to improve the

strength behavior of sand, and the results indicated that the UCS increased with gellan gum content. The UCS of 2% gellan gum-treated sand was around 180 kPa. Meanwhile, the residual strength of hydrogel-impregnated sand increased with the increase of sodium alginate content, and hydrogel-impregnated sand with 0.4% sodium alginate content had a residual strength of 100 kPa. This is in agreement with the fact that the gellan gum contents had a positive effect on residual strength of gellan gum-treated sand [12].

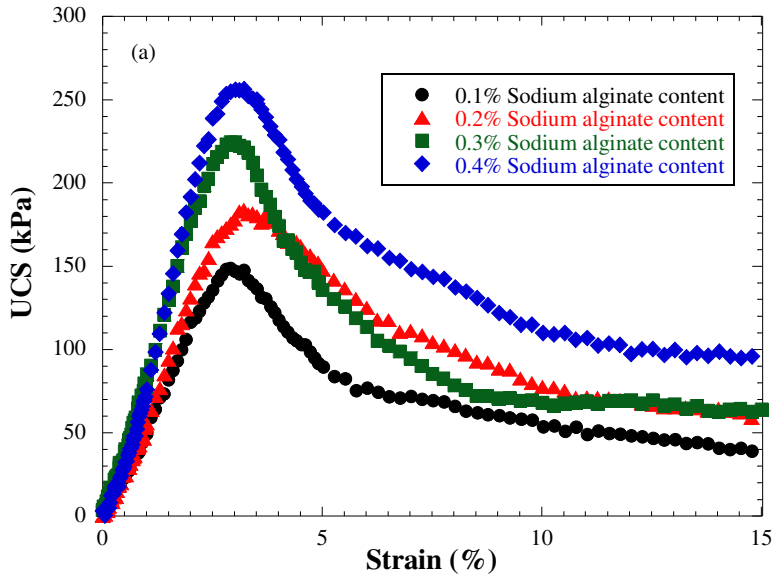

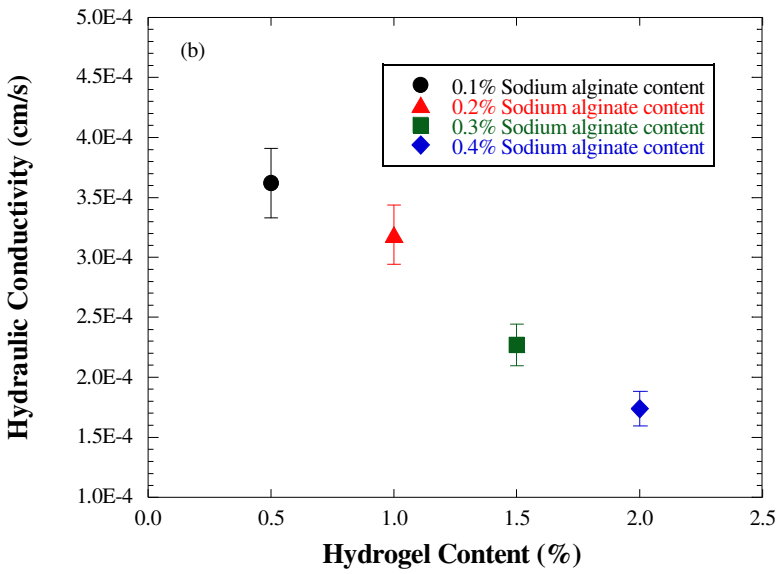

Figure 4. The effect of sodium alginate content on (a) stress-strain curve; (b) hydraulic conductivity of hydrogel-impregnated sand.

The hydraulic conductivity of hydrogel-impregnated sand at different sodium alginate contents was investigated in this study. As shown in Figure 4 (b), the higher the sodium alginate content, the lower the hydraulic conductivity of hydrogel-impregnated sand. The hydraulic conductivity decreased from an untreated condition (~10^{-2} cm/s) to hydrogel-impregnated sand with 0.4% sodium alginate content (~1.8×10^{-4} cm/s), indicating that the void spaces between sand particles were filled and cemented by the inclusion of hydrogel.

Effect of curing temperature on strength improvement of hydrogel-impregnated sand

Four different curing conditions were selected to investigate the effect of curing temperature on the UCS of hydrogel-impregnated sand. Figure 5 shows the stress-strain curve of hydrogel-impregnated sand with 0.4% sodium alginate content at different curing temperatures. The wet condition means that the samples were tested without curing. It can be shown that the performance of stress-strain hydrogel-impregnated sand was significantly affected by the curing temperature. The highest UCS was around 430 kPa at 50^0C oven-dried curing condition, and the lowest one was 160 kPa at 100^0C oven-dried curing condition. Chang et al. [12] studied the strength behaviors of gellan gum-treated sand under different curing conditions. They reported that the UCS of the air-dried sample was higher than that of the wet samples. This is related to the remaining sodium ions in the wet sample degrading/decrosslinking the Ca-alginate over time during the air-dry process over 28 days.

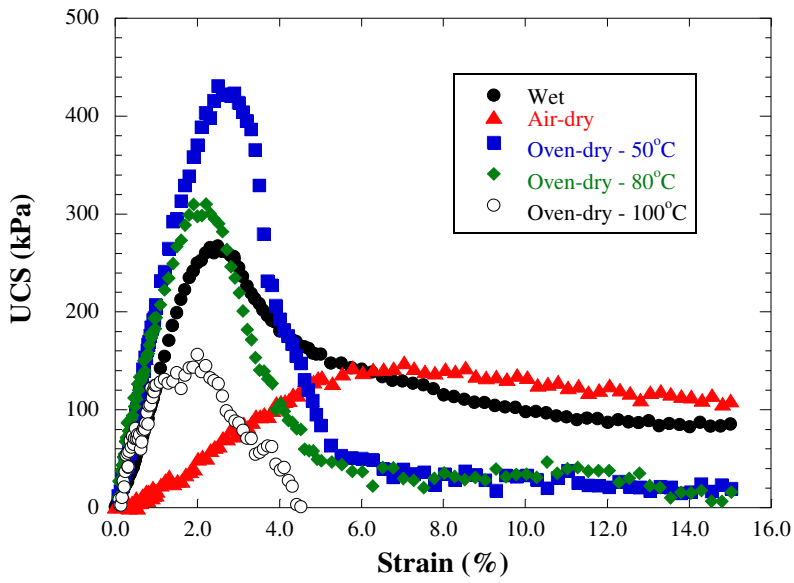

Figure 5. The stress-strain curve of hydrogel-impregnated sand under different curing conditions.

The failure modes of hydrogel-impregnated sand at different curing temperatures are shown in Figure 6. In the case of the wet condition, the sample did not completely break after peak strength and was still cemented by hydrogel, achieving a residual strength of 90 kPa at 15% strain. The failure sample exhibited a shear zone failure mode as shown in Figure 6 (a). An X-shape shear band and several small cracks appeared in the failure sample. Asghari et al. [39] found this similar failure mode for lime-cemented sand. Figure 6 (b) shows the failure sample after 28 days of air-dried conditions. The sample failed in a barreling or drum shape and no cracks were identified, indicating a uniform status of the sample. This is consistent with the result from the stress-strain curve in Figure 5. The air-dried sample presented a superior ductility, and the failure strain was around 7%, with 100 kPa residual strength at 15% strain. Plé and Lê [40] reported that the fiber-reinforced silty clay soil presented a drum shape failure mode, which indicated that the strain localization is prevented by the presence of the fibers. When the

hydrogel-impregnated sample was cured at higher temperatures, the ductility and strength significantly changed. Figure 6 (c) shows the failure sample at 50°C curing temperature, and the sample exhibited a shear failure mode. Meanwhile, the peak strength reached around 430 kPa, but the stress reduced dramatically after peak stress. The residual strength was around 20 kPa at 15% failure strain. When the curing temperature increased to 100°C, the failure strain reduced to around 2.0% and the peak stress reduced to 160 kPa. The sample was brittle and weak with no residual stress. The top of the sample was broken and the failed portion became loose sand as shown in Figure 6 (d).

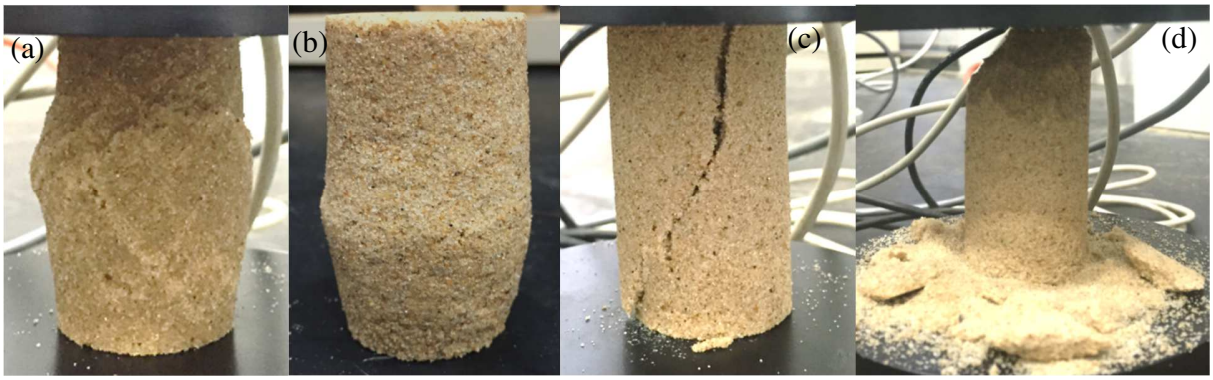

Figure 6. The failure mode of hydrogel-impregnated sand under (a) wet condition; (b) air-dry condition; (c) 50^0C oven-dried condition; (d) 100^0C oven-dried condition.

The SEM images of untreated sand and hydrogel-impregnated sand are shown in Figure 7. The untreated sand did not have cohesion, and the shape of untreated sand was irregular as shown in Figure 7 (a). The image of hydrogel impregnated sand under wet condition is shown in Figure 7 (b). The hydrogel uniformly warped the sand particles and cemented them together, resulting in the reduction of void space. This is consistent with the results of hydraulic conductivity in Figure 4 (b). The hydrogel connection shrank in size after the hydrogel-

impregnated sample cured at 50°C as shown in Figure 7 (c). However, the strength of 50°C dried sample increased which may be because the hydrogel becomes a solid material during the drying process.

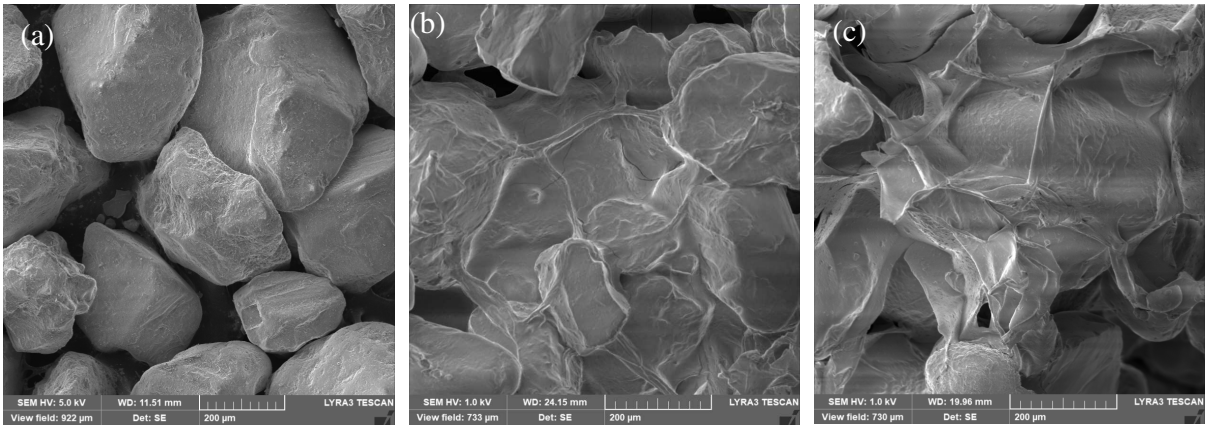

Figure 7. SEM images of a) Untreated Mississippi sand; b) hydrogel-impregnated sand under wet condition; c) hydrogel-impregnated sand under dry condition (50^0C oven dried).

Shear strength of hydrogel-impregnated sand

The natural repose angle of Mississippi sand is shown in Figure 8 (a), which was around 32°. The consolidated and undrained triaxial tests were conducted on hydrogel-impregnated sand with 0.4% sodium alginate, and three different confining pressures (100 kPa, 200 kPa and 400 kPa) were selected. Figure 8 (b) shows the Mohr circle curves and failure envelopes obtained from triaxial compression strength tests on hydrogel-impregnated samples. The test results show that the cohesion and friction angle of hydrogel-impregnated sand were 150 kPa and 16°, respectively. Sandy soil is well-known as cohesionless soil. The gelation connection provided by hydrogel enhanced the connection between sand particles and improved the cohesion of sandy soil. Li et al.

254 [41] investigated the shear strength of MICP-treated sand (0.18 M Ca) and found that the
255 cohesion of MICP-treated sand increased to 20 kPa, which was much lower than that of
256 hydrogel-impregnated sand, and the friction angle of MICP-treated sand was similar to that of
257 hydrogel-impregnated sand.

258

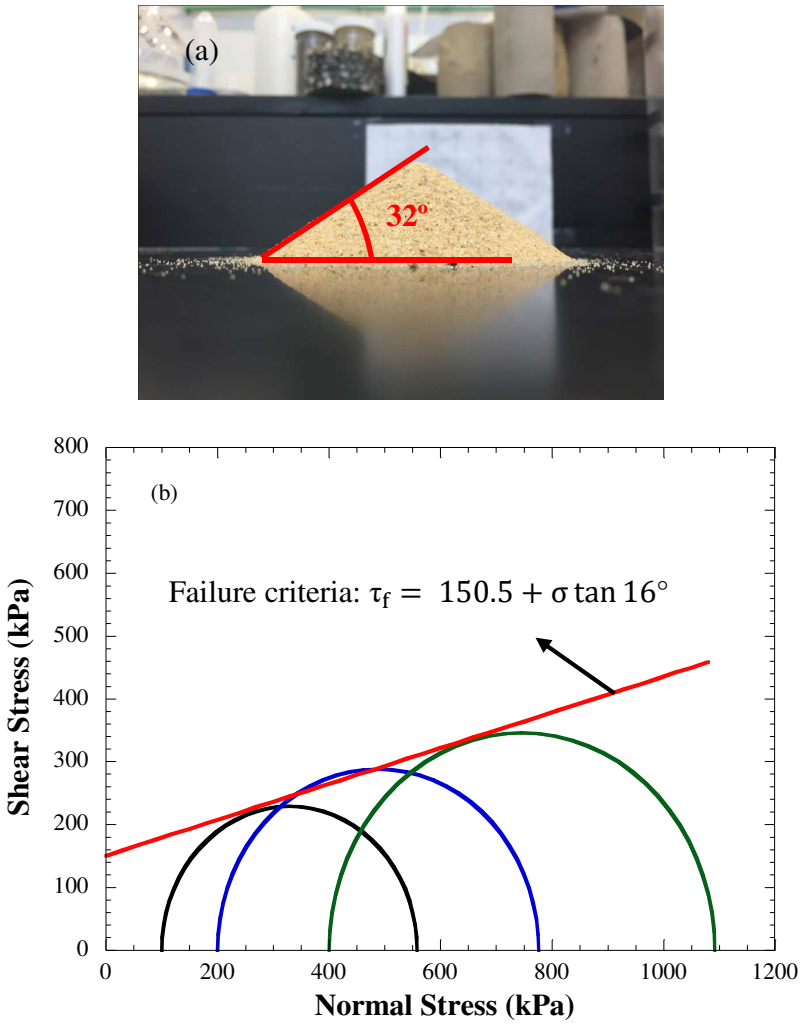

259

260

261 Figure 8. (a) The natural repose angle of Mississippi sand; (b) Mohr circle and failure envelope
262 of hydrogel-impregnated sand with 0.4% sodium alginate.

263

Durability Test on Hydrogel-impregnated Sand

The durability of hydrogel-impregnated sand was tested through wet-dry and freeze-thaw cycles. The effect of wet-dry and freeze-thaw cycles on the UCS of hydrogel-impregnated sand is shown in Figure 9. The samples used for the durability tests were hydrogel-impregnated samples with 0.4% sodium alginate content at a curing temperature of 50°C. It was found that no significant difference for the samples subjected to 3 wet-dry or freeze-thaw cycles. After 3 cycles, the UCS of hydrogel-impregnated sand started to decrease with the increase of wet-dry or freeze-thaw cycles. After 12 wet-dry or freeze-thaw cycles, 60% of the original UCS of the hydrogel-impregnated sand still remained. Kampala et al. [42] used fly-ash to reinforce clay soil, and the UCS reduced over 50% after 6 wet-dry cycles. Chang et al. [12] studied the strength behavior of 2% gellan gum-treated sand and found that the UCS dropped dramatically from 435 kPa (dry condition) to 45 kPa (re-submerged condition). This result indicated that the gellan gum-treated sand was not recoverable once the gellan gum gel is condensed through dehydration. Eskişar et al. [43] found that cement-treated clay reduced 50% in strength after 5 freeze-thaw cycles. With these studies, it is indicated that the Ca-alginate hydrogel has a superior durability performance.

However, the natural environment contains many micro-organisms that may have an impacted the stability of Ca-alginate impregnated sand. Studies have concluded that the decreased mechanical strength of Ca-alginate is due to the entrapped growing microorganism [44,45]. Therefore, the effects of microorganisms on the mechanical properties of hydrogel-impregnated samples need to be studied further.

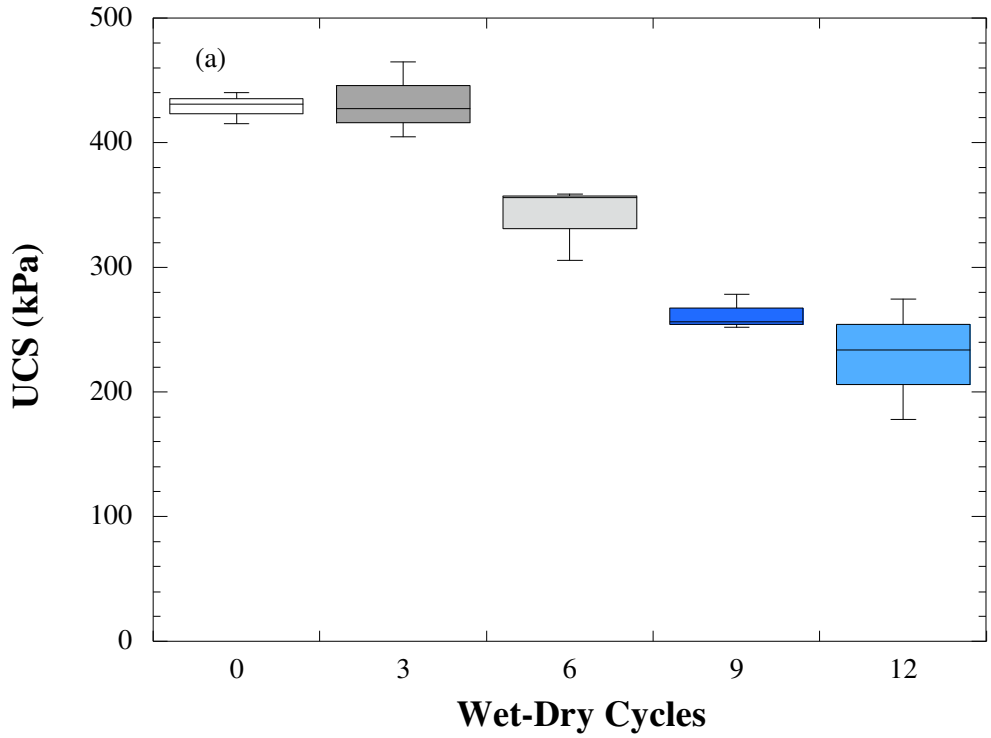

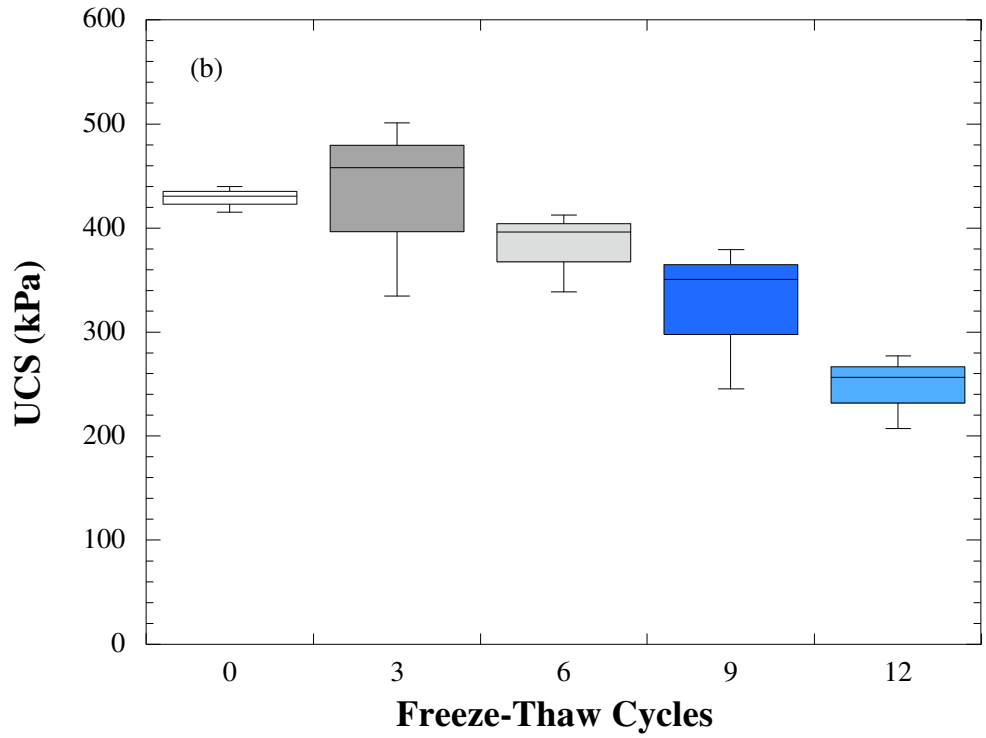

Figure 9. The effect of wet-dry (a) and freeze-thaw (b) cycles on unconfined compressive strength of hydrogel-impregnated sand

Conclusions

As an environmentally friendly material used for sandy soil improvement, the hydrogel-impregnated sand achieved a relatively high strength even at low concentrations of hydrogel. The effects of reaction time, sodium alginate content, and curing temperature on mechanical behaviors of hydrogel-impregnated sand were studied through unconfined compression tests, falling head permeability tests, consolidated and undrained triaxial tests, scanning electron microscopy, and durability tests. The optimum reaction time and curing temperature of hydrogel-impregnated sand were found to be 3 days and 50°C, respectively. The UCS tended to increase with more sodium alginate content, but hydraulic conductivity decreased with the sodium alginate content. The UCS of hydrogel-impregnated sand at 0.4% sodium alginate content reached 430 kPa and presented to be the optimum mixture ratio. The hydrogel-impregnated sand showed a significant improvement in the cohesion of the sand particles. The results showed that the cohesion and friction angle of hydrogel-impregnated sand at 0.4% sodium alginate content were 150 kPa and 16º, respectively. In addition, the stress-strain curves of hydrogel-impregnated sand indicated that the ductility of hydrogel-impregnated sand was significantly improved compared to traditional cementitious methods. Moreover, the results of durability tests indicated that approximately 60% of original UCS of hydrogel-impregnated sand still remained after 12 wet-dry and freeze-thaw cycles.

Acknowledgments

This work was supported by the National Science Foundation Grant No. 1531382 and MarTREC. The third author expressed the support from China Scholarship Council Program (No. 201708505131).

References

[1] N. Latifi, S. Horpibulsuk, C.L. Meehan, M.Z. Abd Majid M, M.M. Tahir, E.T. Mohamad. Improvement of problematic soils with biopolymer—an environmentally friendly soil stabilizer. J. Mater. Civ. Eng., 29 (2) (2016), pp. 04016204.

[2] R. Horn, H. Domżżał, A. Słowińska-Jurkiewicz, C. Van Ouwerkerk. Soil compaction processes and their effects on the structure of arable soils and the environment. Soil Till. Res., 35(1-2) (1995), pp. 23-36.

[3] M.W. Bo, A. Arulrajah, S. Horpibulsuk, M. Leong, M.M. Disfani. Densification of Land Reclamation Sands by Deep Vibratory Compaction Techniques. J. Mater. Civ. Eng., 26 (8) (2013), pp. 06014016.

[4] Y. Chen. Study of Ground Treatment on Improvement of Pile Foundation Response in Liquefiable Soils. Geotech. Geol. Eng., 35(5) (2017), pp.2219-2226.

[5] S.K. Dash, M. Hussain. Lime stabilization of soils: reappraisal. Journal of materials in civil engineering, 24(6) (2011), pp. 707-714.

[6] S. Horpibulsuk, C. Phetchuay, A. Chinkulkijniwat. Soil stabilization by calcium carbide residue and fly ash. J. Mater. Civ. Eng., 24(2) (2011), pp. 184-193.

[7] N. Cristelo, S. Glendinning, L. Fernandes, A.T. Pinto. Effects of alkaline-activated fly ash and Portland cement on soft soil stabilisation. Acta Geotech., 8(4) (2013), pp. 395-405.

[8] S.H. Chew, A.H.M. Kamruzzaman, F.H. Lee. Physicochemical and engineering behavior of cement treated clays. J. Geotech. Geoenviron. Eng., 130(7) (2004), pp. 696-706.

[9] M. Al-Mukhtar, A. Lasledj, J.F. Alcover. Behaviour and mineralogy changes in lime-treated expansive soil at 20 C. Appl. Clay Sci., 50(2) (2010), pp. 191-198.

[10] C.A. Anagnostopoulos. Strength properties of an epoxy resin and cement-stabilized silty clay soil. Appl. Clay Sci., 114 (2015), pp. 517-529.

[11] C. Bu, K. Wen, S. Liu, U. Ogbonnaya, L. Li. Development of bio-cemented constructional materials through microbial induced calcite precipitation. Mater. Struct., 51(1) (2018), pp. 30.

[12] I. Chang, A.K. Prasidhi, J. Im, G.C. Cho. Soil strengthening using thermo-gelation biopolymers. Constr. Build. Mater., 77 (2015), pp. 430-438.

[13] J.T. DeJong, B.M. Mortensen, B.C. Martinez, D.C. Nelson. Bio-mediated soil improvement. Ecol. Eng., 36(2) (2010), pp. 197-210.

[14] G. Blanck, O. Cuisinier, F. Masrouri. Soil treatment with organic non-traditional additives for the improvement of earthworks. Acta Geotech., 9(6) (2014), pp. 1111-1122.

[15] N. Latifi, A. Marto, A. Eisazadeh. Physicochemical behavior of tropical laterite soil stabilized with non-traditional additive. Acta Geotech., 11(2) (2015), pp. 433-443.

[16] D. Bernardi, J.T. DeJong, B.M. Montoya, B.C. Martinez. Bio-bricks: Biologically cemented sandstone bricks. Constr. Build. Mater., 55 (2014), pp. 462-469.

[17] Q. Zhao, L. Li, C. Li, M. Li, F. Amini, H. Zhang. Factors affecting improvement of engineering properties of MICP-treated soil catalyzed by bacteria and urease. J. Mater. Civ. Eng., 26(12) (2014), pp. 04014094.

[18] M. Li, K. Wen, Y. Li, L. Zhu. Impact of Oxygen Availability on Microbially Induced Calcite Precipitation (MICP) Treatment. Geomicrobiol. J., 35(1) (2018), pp. 15-22.

[19] K. Wen, C. Bu, S. Liu, Y. Li, L. Li. Experimental investigation of flexure resistance performance of bio-beams reinforced with discrete randomly distributed fiber and bamboo. Constr. Build. Mater., 176 (2018), pp. 241-249.

[20] I. Chang, J. Im, G.C. Cho. Geotechnical engineering behaviors of gellan gum biopolymer treated sand. Can. Geotech. J., 53(10) (2016), pp. 1658-1670.

[21] D. Seliktar. Designing cell-compatible hydrogels for biomedical applications. Science, 336(6085) (2012), pp. 1124-1128.

[22] Y.S. Zhang, A. Khademhosseini. Advances in engineering hydrogels. Science, 356(6337) (2017), pp. eaaf3627.

[23] X. Zhao (2014). Multi-scale multi-mechanism design of tough hydrogels: building dissipation into stretchy networks. Soft Matter, 10(5) (2014), pp. 672-687.

[24] J.P. Gong, Y. Katsuyama, T. Kurokawa, Y. Osada. Double‐network hydrogels with extremely high mechanical strength. Adv. Mater., 15(14) (2003), pp. 1155-1158.

[25] J.Y. Sun, X. Zhao, W.R. Illeperuma, O. Chaudhuri, K.H. Oh, D.J. Mooney, J.J. Vlassak, Z. Suo. Highly stretchable and tough hydrogels. Nature, 489(7414) (2012), pp. 133.

[26] K. Dey, P. Roy. Degradation of chloroform by immobilized cells of Bacillus sp. in calcium alginate beads. Biotechnol. Lett., 33 (2011), pp. 1101–1105.

[27] J. Wang, A. Mignon, D. Snoeck, V. Wiktor, S. Van Vliergerghe, N. Boon, N. De Belie. Application of modified-alginate encapsulated carbonate producing bacteria in concrete: a promising strategy for crack self-healing. Front. Microbiol., 6 (2015), pp. 1088.

[28] ASTM C136/C136M-14 (2014) Standard Test Method for Sieve Analysis of Fine and Coarse Aggregates, ASTM International, West Conshohocken, PA.

[29] K.Y. Lee, D.J. Mooney. Alginate: properties and biomedical applications. Prog. Polym. Sci., 37(1) (2012), pp. 106-126.

[30] ASTM D2166/D2166M-13 (2013) Standard test method for unconfined compressive strength
of cohesive soil. ASTM International, West Conshohocken, PA.

[31] ASTM-D5084-16a (2016) Standard test methods for measurement of hydraulic conductivity of saturated porous materials using a flexible wall permeameter. ASTM International, West Conshohocken, PA.

[32] ASTM D2434-68 (2006) Standard Test Method for Permeability of Granular Soils (Constant Head). ASTM International, West Conshohocken, PA.

[33] ASTM-D560 (2016) Standard Test Methods for Freezing and Thawing Compacted Soil Cement Mixtures. ASTM International, West Conshohocken, PA.

[34] ASTM-D559 (2015) Standard Test Methods for Wetting and Drying Compacted Soil-Cement

Mixtures. ASTM International, West Conshohocken, PA.

[35] M.S. Shoichet, R.H. Li, M.L. White, S.R. Winn. Stability of hydrogels used in cell encapsulation: An in vitro comparison of alginate and agarose. Biotechnol. and bioeng., 50(4) (1996), pp. 374-381.

[36] J.A. Rowley, G. Madlambayan, D.J. Mooney. Alginate hydrogels as synthetic extracellular matrix materials. Biomaterials, 20(1) (1999), pp. 45-53.

[37] J.C. Breger, B. Fisher, R. Samy, S. Pollack, N.S. Wang, I. Isayeva. Synthesis of "click" alginate hydrogel capsules and comparison of their stability, water swelling, and diffusion properties with that of Ca^{+2} crosslinked alginate capsules. J. Biomed. Mater. Res. B, 103(5) (2015), pp. 1120-1132.

[38] N.C. Consoli, R.C. Cruz, M.F. Floss, L. Festugato. Parameters controlling tensile and compressive strength of artificially cemented sand. J. Geotech. Geoenviron. Eng., 136(5) (2009), 759-763.

[39] E. Asghari, D.G. Toll, S.M. Haeri. Triaxial behaviour of a cemented gravely sand, Tehran alluvium. Geotech. Geol. Eng., 21(1) (2003), pp. 1-28.

[40] O. Plé, T.N.H. Lê. Effect of polypropylene fiber-reinforcement on the mechanical behavior of silty clay. Geotext. Geomembranes, 32 (2012), pp. 111-116.

[41] M. Li, L. Li, U. Ogbonnaya, K. Wen, A. Tian, F. Amini. Influence of fiber addition on mechanical properties of MICP-treated sand. J. Mater. Civ. Eng., 28(4) (2015), pp. 04015166.

[42] A. Kampala, S. Horpibulsuk, N. Prongmanee, A. Chinkulkijniwat. Influence of wet-dry cycles on compressive strength of calcium carbide residue–fly ash stabilized clay. J. Mater. Civ. Eng., 26(4) (2013), pp. 633-643.

[43] T. Eskişar, S. Altun, İ, Kalıpcılar. Assessment of strength development and freeze–thaw performance of cement treated clays at different water contents. Cold Reg. Sci. Technol., 111 (2015), pp. 50-59.

[44] K. Dey, P. Roy. Degradation of chloroform by immobilized cells of Bacillus sp. in calcium alginate beads. Biotechnol. Lett., 33 (2011), pp. 1101–1105.

[45] H. Eikmeier, H.J. Rehm. Stability of calcium-alginate during citric acid production of immobilized Aspergillus niger. Appl. Microbiol. Biotechnol., 26(2) (1987), pp.105-111.